Effective empirical corrections for basis set superposition error in the def2-SVPD basis: gCP and DFT-C

Jonathon Witte, Jeffrey B. Neaton, and Martin Head-Gordon

Articles you may be interested in

Effective empirical corrections for basis set superposition error in the def2-SVPD basis: gCP and DFT-C

Jonathon Witte,[1,2] Jeffrey B. Neaton,[2,3,4] and Martin Head-Gordon[1,5,a]

[1]*Department of Chemistry, University of California, Berkeley, California 94720, USA*
[2]*Molecular Foundry, Lawrence Berkeley National Laboratory, Berkeley, California 94720, USA*
[3]*Department of Physics, University of California, Berkeley, California 94720, USA*
[4]*Kavli Energy Nanosciences Institute at Berkeley, Berkeley, California 94720, USA*
[5]*Chemical Sciences Division, Lawrence Berkeley National Laboratory, Berkeley, California 94720, USA*

With the aim of mitigating the basis set error in density functional theory (DFT) calculations employing local basis sets, we herein develop two empirical corrections for basis set superposition error (BSSE) in the def2-SVPD basis, a basis which—when stripped of BSSE—is capable of providing near-complete-basis DFT results for non-covalent interactions. Specifically, we adapt the existing pairwise geometrical counterpoise (gCP) approach to the def2-SVPD basis, and we develop a beyond-pairwise approach, DFT-C, which we parameterize across a small set of intermolecular interactions. Both gCP and DFT-C are evaluated against the traditional Boys-Bernardi counterpoise correction across a set of 3402 non-covalent binding energies and isomerization energies. We find that the DFT-C method represents a significant improvement over gCP, particularly for non-covalently-interacting molecular clusters. Moreover, DFT-C is transferable among density functionals and can be combined with existing functionals—such as B97M-V—to recover large-basis results at a fraction of the cost. *Published by AIP Publishing.* [http://dx.doi.org/10.1063/1.4986962]

I. INTRODUCTION

In an electronic structure calculation, two forms of basis set errors arise when local basis sets are employed: basis set superposition error (BSSE), which is a consequence of inconsistent treatment of a larger supersystem and its constituent subsystems,[1–3] and intrinsic basis set incompleteness error, the category to which we relegate all remaining basis set errors once BSSE has been removed.[4] Intrinsic incompleteness error arises from the fact that the Schrödinger equation is being solved in just a fraction of the full Hilbert space, and no systematic means of removal—short of simply increasing the number of basis functions—has yet been discovered, though adaptive-basis approaches have shown some promise.[5–10] Basis set superposition error, on the other hand, has a long history within the electronic structure community.[11–20] In the case of distinct non-covalently interacting units, BSSE can be removed by performing fragment calculations within the basis of the full system, i.e., via the counterpoise correction (CP) first introduced by Boys and Bernardi.[2]

The standard counterpoise correction has two principal shortcomings. First, it requires a partitioning of the full system into a number of fragments, $N_{\text{fragments}}$; for some systems, such as those with simple bimolecular interactions, this partitioning is straightforward, but for many interesting systems—such as those involving substantial intramolecular interactions—it is not. Second, although in principal a good approximation to counterpoise-corrected results may be obtained with

minimal extra effort via standard energy decomposition analyses,[21,22] in practice the CP correction often ends up being quite computationally demanding, whereas an uncorrected binding energy requires only one calculation in the full supersystem basis, a counterpoise-corrected one requires $N_{\text{fragments}} + 1$ such calculations.

The issues of partitioning and the inability of the CP scheme to address intramolecular BSSE were first addressed by Galano and Alvarez-Idaboy with an atom-by-atom counterpoise correction;[23] Jensen later generalized this into the atomic counterpoise (ACP-n) approach.[24] In the ACP-n scheme, BSSE is estimated as a sum of atomic BSSEs, where each atomic BSSE is calculated by considering basis functions up to n bonded atoms away. This approach has shown some promise in addressing intramolecular BSSE, though it suffers from the same partitioning problem as CP when ambiguous bonding patterns are involved—e.g., in transition states and hydrogen-bonded systems—and the computational complexity of the method is unchanged.

More recently, there have been attempts to develop empirical models for BSSE, as such approaches can potentially address both the partitioning and complexity issues. The first such model was proposed six years ago by Faver and Merz,[25,26] who constructed the so-called "proximity functions" for molecular fragments from atomic pairs. Since the targets for this method are large biomolecules, the parameters are trained on a variety of proteinogenic systems. To date, this is the only empirical correction for BSSE developed for correlated wavefunction-based methods. The chief shortfall of the approach lies in its limited transferability; the parameters for modeling typical nonpolar, van der Waals-driven

---

[a]Electronic mail: mhg@cchem.berkeley.edu

interactions are significantly different than those used for modeling hydrogen bonding.

Kruse and Grimme more recently introduced the so-called geometrical counterpoise (gCP) scheme,[27] which was later combined with the DFT-D3(BJ)[28,29] dispersion correction and either an explicit—in the form of an additional short-range term—or implicit—in the form of a modified basis set—correction for basis set incompleteness to form the HF-3c, PBEh-3c, and HSE-3c methods.[30–32] The gCP scheme loosely resembles the proximity function approach of Faver and Merz, in as much as both methods are strictly pairwise atomic corrections. Unlike the proximity function-based correction, however, gCP has gained considerable traction within the electronic structure community,[33–35] largely due to its low-cost, satisfactory transferability, and ease of use. The gCP approach is utilized in conjunction with very small basis sets—on the order of 6-31G*—and is capable of recovering most of the BSSE in typical systems.

Within this work, we adapt the gCP empirical correction for BSSE to the def2-SVPD basis. We focus exclusively on the def2-SVPD basis set[36,37] due to its good balance of expense and performance; def2-SVPD has low intrinsic incompleteness error relative to other comparable-sized bases,[38] and hence seems to us to be a particularly promising basis set for BSSE correction schemes. In addition, we develop an alternative beyond-pairwise empirical correction for BSSE within density functional theory: DFT-C. The many-body nature of the method accounts for the overcounting concomitant with any pairwise approach and allows DFT-C to treat both large and small systems in a consistent manner. Whereas gCP is developed for use with exceptionally small basis sets, with the aim of providing semi-quantitative results, we demonstrate that DFT-C can recover near-basis-set-limit results at a fraction of the cost, particularly in the case of non-covalent interactions.

II. THEORY AND METHODS

A. gCP

Here, we will briefly summarize the geometrical counterpoise (gCP) correction for BSSE; for further details, see the original study by Kruse and Grimme.[27] At the core of gCP lies a function describing the decay of BSSE on atom A due to the presence of basis functions on atom B a distance r_{AB} away, which we denote $f^{\text{gCP}}_{AB^*}(r_{AB})$. This term is given by

$$f^{\text{gCP}}_{AB^*}(r_{AB}) = c_{AB} \exp\left(-\alpha r^{\beta}_{AB}\right) \tag{1}$$

and includes a multiplicative constant, c_{AB}, as well as a universal decay parameter α and exponent β. The contributions of all atom-ghost pairs are summed up to yield the gCP correction for BSSE,

$$E_{\text{gCP}} = \sigma \sum_A c_A \sum_{B \neq A} f^{\text{gCP}}_{AB^*}(r_{AB}), \tag{2}$$

where c_A are atom-dependent parameters and σ is an overall scaling parameter. In practice, E_{gCP} is just added to the total electronic energy for a given system. The gCP approach is strictly pairwise additive with respect to nuclear centers.

B. Parameterization of gCP

Equations (1) and (2) contain several parameters: multiplicative constants c_{AB}, linear coefficients c_A, decay factors α and β, and an overall scaling factor σ. The pairwise multiplicative constants, c_{AB}, are calculated as

$$c_{AB} = \frac{1}{\sqrt{S_{AB} N^{\text{virt}}_B}}, \tag{3}$$

where N^{virt}_B is the number of virtual orbitals on atom B—given by $N^{\text{virt}}_B = N^{\text{basis functions}}_B - \frac{1}{2} N^{\text{electrons}}_B$—and S_{AB} is a measure of the Slater overlap between atoms A and B. The overlap term is described in detail in the original study;[27] here, we will simply note that it involves an additional linear parameter, η.

The atomic linear coefficients, c_A, are calculated within the gCP approach as "missing energy" terms, i.e., c_A is calculated as the difference in restricted open-shell Hartree-Fock[39] energy between atom A in a target basis (here def2-SVPD) and a large basis, in the presence of an external electric field to populate higher angular momentum functions. We have utilized aug-pc-4 as the large basis.[40–42]

The remaining parameters—three nonlinear (α, β, and η) and one linear (σ)—are obtained by minimizing the error in predicted gCP BSSE relative to Boys-Bernardi BSSE with the B3LYP[43–46] density functional across the S66×8 dataset of intermolecular interactions,[47,48] within the def2-SVPD basis. As in the original work, the most compressed geometries are weighted for this optimization by a factor of 0.5 in order to emphasize equilibrium and long-distance structures.

The optimized set of parameters is provided in the supplementary material; this set of parameters allows the existing gCP approach to be utilized with the def2-SVPD basis set for DFT. Briefly, we mention one particularly interesting aspect of the optimized parameters: the optimal value of η—the parameter controlling atomic overlap in the gCP model—in the def2-SVPD basis is 0.000 01, which suggests that for this particular basis set, the gCP expression can be simplified without degrading performance by simply removing the overlap term. We have verified that this is in fact true; we present in the supplementary material a simpler formulation of gCP for def2-SVPD.

C. DFT-C

In addition to re-parameterizing the gCP method for use with the def2-SVPD basis, we also present a more complex, though physically motivated, geometry-based empirical approximation for BSSE, which will henceforth be referred to as DFT-C. This model is in many ways similar to gCP.[27] At its core lies a term describing the decay of BSSE on atom A due to the presence of basis functions on atom B a distance r_{AB} away, which we denote $f^{\text{DFT-C}}_{AB^*}(r_{AB})$. This term is given by

$$f^{\text{DFT-C}}_{AB^*}(r_{AB}) = c_{AB} \exp\left(-\alpha_{AB} r^2_{AB} + \beta_{AB} r_{AB}\right) \tag{4}$$

and includes a multiplicative constant, c_{AB}, a Gaussian decay parameter, α_{AB}, and an exponential decay parameter, β_{AB}. We expect the decay of BSSE to mirror that of the electron density; the exponential term accounts for the standard decay expression,[49] and the Gaussian term reflects the nature of the basis

functions employed. The DFT-C approach includes both an exponential term and a Gaussian term, with pair-dependent decay factors; these differences set it apart from the gCP core term given in Eq. (1).

In DFT-C, we damp this atomic contribution to BSSE, much as the contribution of gCP is damped in PBEh-3c to potentially address short-r_{AB} issues that can arise in thermochemical problems.[31] We employ the same form of damping function as PBEh-3c,[31]

$$d(r_{AB}) = \frac{1}{1 + k_{1,AB}(r_{AB}/r_{0,AB})^{-k_{2,AB}}}, \quad (5)$$

where $r_{0,AB}$ is the sum of the van der Waals radii of atoms A and B, and $k_{1,AB}$ and $k_{2,AB}$ are parameters that control the precise shape of the damping function. Whereas Grimme et al.[31] set $k_1 = 4$ and $k_2 = 6$ for all pairs of atoms A and B by inspection, we compute them systematically for each atom pair based on the sums of covalent and van der Waals radii such that $d(r_{cov,AB}) = 0.05$ and $d(r_{0,AB}) = 0.95$. Doing so yields $k_{1,AB} = 19$ and $k_{2,AB} = 5.8889[\log(r_{0,AB}/r_{cov,AB})]^{-1}$. Moreover, we propose damping to a finite value, rather than zero, to more accurately reflect the actual short-range behavior of BSSE; after all, BSSE does not simply vanish in the covalent bonding distance regime. Thus, rather than simply multiplying the contribution from Eq. (4) by the damping function in Eq. (5), we define a damped contribution, $g_{AB^*}^{DFT-C}(r_{AB})$, as

$$g_{AB^*}^{DFT-C}(r_{AB}) = d(r_{AB})f_{AB^*}^{DFT-C}(r_{AB}) + (1 - d(r_{AB}))$$
$$\times f_{AB^*}^{DFT-C}(r_{cov,AB}). \quad (6)$$

At long range, this term reduces to $f_{AB^*}^{DFT-C}(r_{AB})$, while at short range, it reduces to a pair-dependent constant, $f_{AB^*}^{DFT-C}(r_{cov,AB})$.

Whereas the gCP correction is strictly pairwise, we incorporate a many-body component into DFT-C. We do so in the following physically motivated though *ad hoc* way, by simply modifying each pairwise contribution by an additional term, $h_{AB^*}(\{A, B, \ldots\})$, which is given by

$$h_{AB^*}(\{A, B, \ldots\}) = \left[1 + \sum_{C \neq A, B} \frac{N_C^{virt}}{N_B^{virt}} \text{ terfc}(r_{AC}, r_{AB})\right.$$
$$\left. \times \text{ terfc}(r_{BC}, r_{AB})\right]^{-1}, \quad (7)$$

where N_B^{virt} is the number of virtual orbitals on atom B—given by $N_B^{virt} = N_B^{basis\ functions} - \frac{1}{2}N_B^{electrons}$ as in gCP, with $N_B^{electrons}$ being the number of electrons on neutral atomic B and $N_B^{basis\ functions}$ corresponding to the number of basis functions centered at atom B—distances are in atomic units, and terfc(x, y) is the attenuator defined by Dutoi and Head-Gordon,[50]

$$\text{terfc}(x, y) = 1 - \frac{1}{2}\left[\text{erf}(x + y) + \text{erf}(x - y)\right]. \quad (8)$$

This additional correction, $h_{AB^*}(\{A, B, \ldots\})$, addresses the nonzero overlap between the Hilbert space of atom B and the Hilbert spaces of all atoms $C \neq A, B$. As more and more atoms are added in the vicinity of atoms A and B, the contribution of the ghost functions centered at B to the atomic
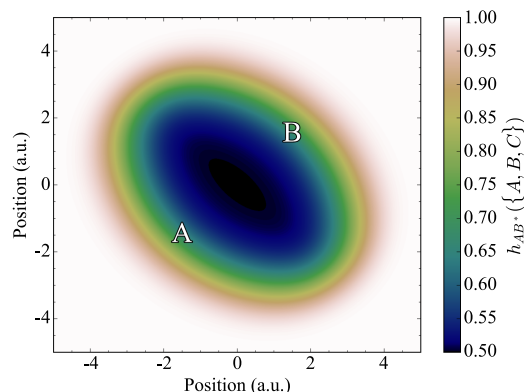

FIG. 1. Visualization of how adding a third atom C impacts the contribution of basis functions centered at B to the BSSE on atom A, as per $h_{AB^*}(\{A, B, C\})$. When atom C is sufficiently far away from A and B (lighter areas), the model reduces to a pairwise approach. In this example, C and B are assumed to have the same number of virtual orbitals, and A and B are located at (−1.5 a.u., −1.5 a.u.) and (1.5 a.u., 1.5 a.u.), respectively.

BSSE of A should decrease; eventually, once the space is saturated, adding additional atoms (i.e., ghost functions) does not change the BSSE of atom A. This phenomenon is not captured by a strictly pairwise approach. The many-body correction we employ is visualized for a planar 3-atom system in Fig. 1.

The final form of the DFT-C correction for BSSE is given by

$$E_{DFT-C} = \sigma \sum_A c_A \sum_{B \neq A} g_{AB^*}^{DFT-C}(r_{AB}) h_{AB^*}(\{A, B, \ldots\}), \quad (9)$$

where σ is an overall scaling coefficient, c_A is a linear coefficient that modifies the contributions of ghost functions on all atoms B to the BSSE on A, and the damped pairwise contribution, $g_{AB^*}^{DFT-C}(r_{AB})$, and many-body correction, $h_{AB^*}(\{A, B, \ldots\})$ are defined in Eqs. (6) and (7), respectively. With the exception of the many-body term, this expression for the DFT-C energy is mathematically similar to that for gCP—cf. Eqs. (9) and (2).

D. Parameterization of DFT-C

As can be seen from Eq. (9), DFT-C has a large number of parameters. For each unique set of atom A and ghost functions centered at atom B, there are exponential and Gaussian decay parameters, α_{AB} and β_{AB}, and there is a multiplicative constant, c_{AB}. These parameters are obtained by generating BSSE curves for neutral atomic pairs AB^* using a form of local spin-density approximation (LSDA), SPW92,[51–54] in the def2-SVPD basis. For each unique atom A and corresponding ghost atom B, we perform a least squares fit on a log BSSE curve generated over the range $[r_{cov,AB}, 5r_{cov,AB}]$ in units of 0.1 a_0. To avoid overemphasizing the long-distance regime—where the atomic BSSE is nearly zero, and hence the logarithm of the BSSE is very large in magnitude—we weight each point by the inverse of the logarithm of the BSSE at each distance. The viability of this approach is demonstrated in Fig. 2 for the neon component of neon-argon BSSE. The DFT-C method does a reasonable job of capturing BSSE throughout the entire distance regime, yielding an root-mean-square error (RMSE) of 0.002 kcal/mol.
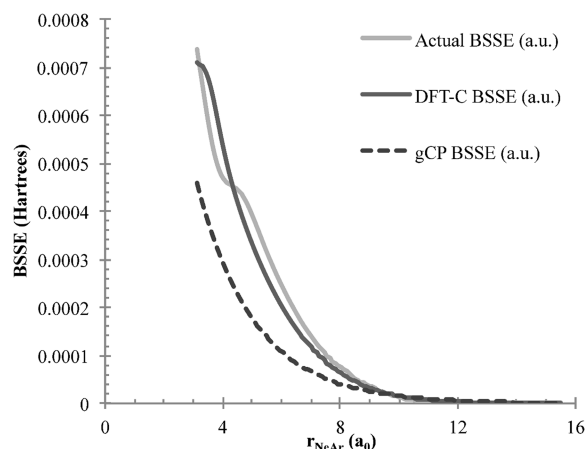
FIG. 2. Dependence of actual and predicted neon atom SPW92/def2-SVPD BSSEs on distance to argon ghost functions.

Note that gCP RMSE for this system is an order of magnitude larger; the lack of a many-body term in gCP necessitates the systematic underprediction of pairwise atomic BSSEs. For pairs AB^* where the Gaussian decay parameter α_{AB} optimizes to a negative value, we set $\beta_{AB} = 0$ and re-optimize, so as to avoid divergence in the large-r_{AB} limit.

We have parameterized all 1296 combinations of the first 36 elements of the periodic table in this manner; the resulting c_{AB}, α_{AB}, and β_{AB} are tabulated in the supplementary material. In the cases of manganese, iron, and cobalt, we have taken averages of the BSSEs for the two competing spin states. For elements heavier than krypton, we propose using the parameters from 4th-row analogues, as is done in gCP.

The linear coefficients, c_A, in Eq. (9) are all unity, with the exception of those for hydrogen, carbon, nitrogen, and oxygen, which are fit via least-squares regression of DFT-C predicted BSSEs to actual BSSEs at the SPW92/def2-SVPD level across the S66 dataset of intermolecular interactions.[47] The overall scaling parameter, σ, is by definition unity for LSDA and is allowed to vary for different density functionals. We have optimized σ for several generalized gradient approximations (GGAs) and meta-GGAs, again by minimizing the root-mean-square error (RMSE) across BSSEs in S66, using the pairwise parameters (c_{AB}, α_{AB}, and β_{AB}) and linear coefficients (c_A) obtained at the LSDA level. For GGA functionals, the optimal value of σ is approximately 0.9, while for meta-GGA functionals, it is slightly lower, near 0.85. We thus propose

using $\sigma = 1$ for LSDA, $\sigma = 0.9$ for GGAs, and $\sigma = 0.85$ for meta-GGAs.

Ultimately, almost all of the parameters associated with the DFT-C method are obtained from toy systems—neutral atom-ghost pairs—at the LSDA level. Four linear coefficients are trained on S66 BSSEs, also at the LSDA level, and for non-LSDA density functionals, we allow for one scaling parameter, which is trained on S66 BSSEs. An implementation of this method within the Python programming language is provided in the supplementary material. In practice, the DFT-C correction is applied in the same manner as gCP: the term from Eq. (9) is simply added to the total electronic energy for a given system.

E. Datasets and computational details

To assess the performance of the gCP and DFT-C methods, we employ a subset of the comprehensive database assembled by Mardirossian and Head-Gordon.[55] The subset we utilize contains 3402 data points distributed over 48 distinct datasets. These smaller constituent datasets are classified according to five distinct datatypes: NCED (easy non-covalent interactions of dimers), NCEC (easy non-covalent interactions of clusters), NCD (difficult non-covalent interactions of dimers), IE (easy isomerization energies), and RG10 (binding curves of rare gas dimers). Unlike "easy" interactions, "difficult" interactions are characterized by strong correlation or self-interaction error. A summary of datatypes may be found in Table I.

In addition to the version of LSDA on which DFT-C is parameterized—SPW92[51–54]—we consider in this study three GGA and three meta-GGA functionals. At the GGA level, we examine a pure functional, PBE;[102] a global hybrid, B3LYP;[43–46]—the functional with which gCP is parameterized—and a range-separated hybrid, ωB97X-V.[103] At the meta-GGA level, we test a pure functional, B97M-V;[104] a global hybrid, M06-2X;[105] and a range-separated hybrid, ωB97M-V.[55]

All density functional calculations are performed in the def2-SVPD basis.[36,37] A fine Lebedev integration grid of 99 radial shells—each with 590 angular points—is used to compute semi-local components of exchange and correlation, while non-local correlation in the VV10-containing functionals is calculated with the coarser SG-1 grid.[106] All calculations are performed within a development version of Q-Chem 4.4.[107]

TABLE I. Summary of datatypes. For more details, see Ref. 55.

Datatype	No.	Constituent datasets	References
NCED	1744	S66, A24, DS14, HB15, HSG, NBC10, S22, X40, A21 × 12, BzDC215, HW30, NC15, S66 × 8, 3B-69-DIM, AlkBind12, CO2Nitrogen16, HB49, Ionic43	47, 48, and 56–77
NCEC	243	H2O6Bind8, HW6Cl, HW6F, FmH2O10, Shields38, SW49Bind345, SW49Bind6, WATER27, H2O20Bind4, 3B-69-TRIM, CE20, H2O20Bind10	71 and 78–87
NCD	91	TA13, XB18, Bauza30, CT20, XB51	88–92
IE	755	AlkIsomer11, Butanediol65, ACONF, CYCONF, Pentane14, SW49Rel345, SW49Rel6, H2O16Rel5, H2O20Rel10, H2O20Rel4, Melatonin52, YMPJ519	79, 81–85, and 93–100
RG10	569	RG10	101

III. RESULTS AND DISCUSSION

In this study, we have developed two geometry-based empirical corrections for BSSE in the def2-SVPD basis: gCP and DFT-C. This particular basis was chosen based on its low intrinsic basis set incompleteness error; BSSE-corrected results obtained within this basis are quite near the basis set limit. This is illustrated in Fig. 3, wherein root-mean-square errors (RMSEs) for B97M-V with (CP) and without (noCP) counterpoise correction against B97M-V/def2-QZVPPD across the various non-covalent datatypes of Table I are shown. Within the def2-SVP basis, even when BSSE is removed (i.e., the CP SVP specification in Fig. 3), the remaining basis set incompleteness error is quite large—significantly larger than method errors for typical density functionals. This indicates that the def2-SVP basis is not suitable for a high-accuracy BSSE correction scheme; its utility would ultimately be contingent on significant cancellation of method and basis set errors. On the other hand, intrinsic incompleteness error in the def2-SVPD basis is quite small, and so a BSSE correction scheme developed in this basis can, in principle, allow for quantitative reproduction of large-basis results.

In addition to developing the DFT-C method, we have also parameterized the existing gCP scheme within the def2-SVPD basis for comparison. The first of these assessments is shown in Fig. 4, wherein we have plotted for the three non-covalent datatypes from Table I normalized

SPW92

FIG. 4. Normalized root-mean-square errors (NRMSEs) of gCP and DFT-C predicted BSSEs versus Boys and Bernardi BSSEs at the LSDA level of DFT in the def2-SVPD basis. The datatypes NCED, NCD, and NCEC are defined in Table I. The normalized root-mean-square error is obtained by dividing the RMSE by the mean reference value in the dataset, as described in the text. Direct use of LSDA/def2-SVPD without any correction would result in 100% NRMSE.

root-mean-square errors (NRMSEs) for DFT-C and gCP predicted BSSEs at the LSDA level of DFT. The normalized RMSE is simply the RMSE divided by the mean of the reference data, and hence provides a measure of relative error. Its use facilitates comparison between NCED and NCEC since the energy scales of those two datatypes differ by more than an order of magnitude.

Within Fig. 4, it is evident that both gCP and DFT-C reproduce Boys-Bernardi BSSEs at the LSDA level reasonably well; either correction is a substantial improvement over no correction. The performance of DFT-C on molecular dimers is particularly promising, as is its consistency across the various datatypes: the lowest DFT-C NRMSE in SPW92 is 25%, for NCED, and the highest is 33%, for NCD. On the other hand, the performance of gCP is quite variable; the method boasts an exceptionally low NRMSE of 19% across NCEC, but a significantly worse NRMSE of 56% for NCD. Neither correction can be considered as a quantitative replacement for the full counterpoise correction.

This same sort of comparison is made for three popular GGA functionals in Fig. 5. Therein, NRMSEs for DFT-C and gCP BSSEs versus actual BSSEs obtained with a pure functional (PBE), a global hybrid (B3LYP), and a range-separated hybrid with non-local correlation (ωB97X-V) may be found. It is clear that for all three density functionals, both DFT-C and gCP are quite consistent with regard to their performances across the various datatypes. Moreover, comparing with Fig. 4, this consistency extends across the LSDA-GGA gap for DFT-C, which bodes well for its transferability.

This same level of consistency is not seen for gCP, however, whereas gCP reproduces LSDA cluster BSSEs with unparalleled accuracy, the method is not nearly as good for clusters at the GGA level: the gCP NRMSE across NCEC in ωB97X-V is more than double that in SPW92. This is a

RMSE (kcal/mol)

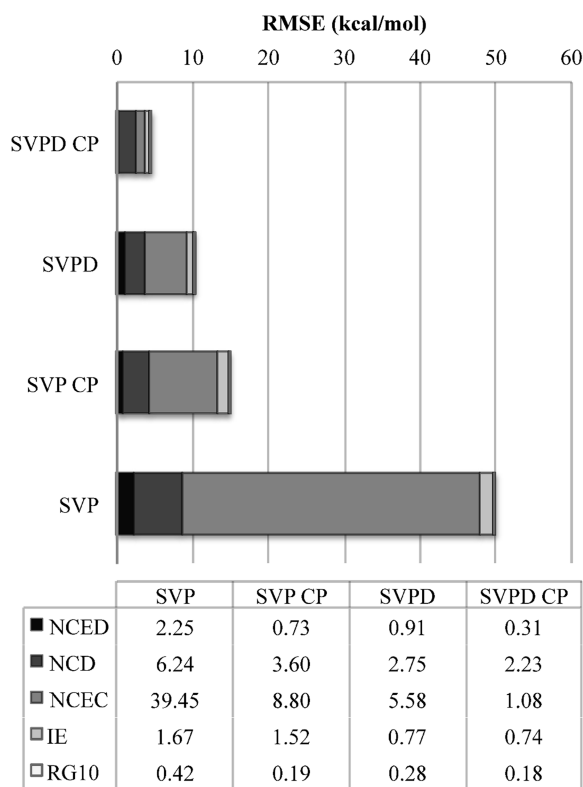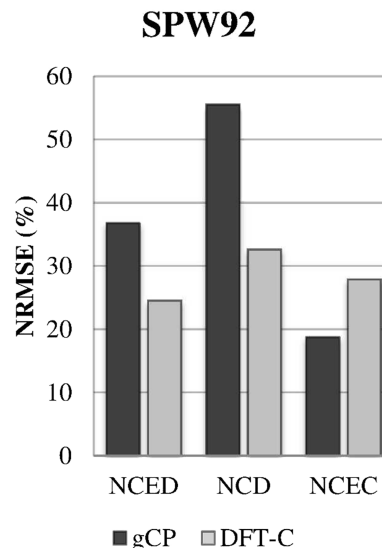|	SVP	SVP CP	SVPD	SVPD CP
■ NCED	2.25	0.73	0.91	0.31
■ NCD	6.24	3.60	2.75	2.23
▦ NCEC	39.45	8.80	5.58	1.08
▤ IE	1.67	1.52	0.77	0.74
▢ RG10	0.42	0.19	0.28	0.18

FIG. 3. Root-mean-square errors of B97M-V with (CP) and without (noCP) the Boys-Bernardi correction for BSSE in two small basis sets relative to B97M-V in the def2-QZVPPD basis, near the basis set limit. SVP and SVPD correspond to def2-SVP and def2-SVPD, respectively. Methods in the chart are ordered from lowest overall RMSE at the top to highest overall RMSE at the bottom. A table of values is provided below the chart to facilitate quantitative comparison.
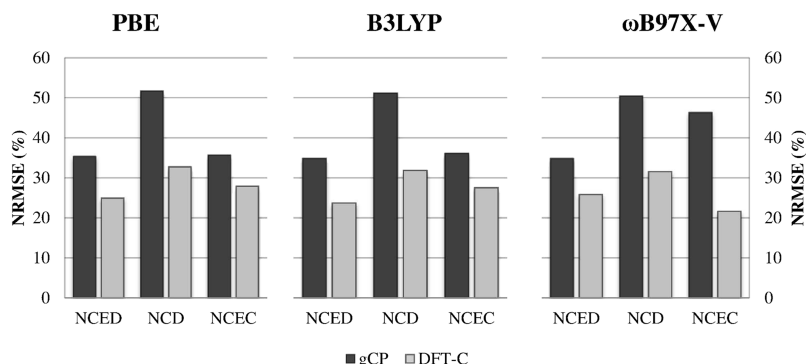
FIG. 5. Normalized root-mean-square errors (NRMSEs) of gCP and DFT-C predicted BSSEs versus Boys and Bernardi BSSEs for three GGA density functionals in the def2-SVPD basis. For further details, see Fig. 4.

consequence of the fact that gCP tends to overestimate BSSE in molecular clusters, and BSSEs obtained at the LSDA level are on average larger than those at the GGA level. The exceptional performance of gCP on SPW92 cluster BSSEs may thus be understood to be largely a consequence of the offsetting of these two phenomena.

It is also evident from Fig. 5 that at the GGA level, DFT-C affords significant gains over gCP regardless of datatype or density functional. This is quite promising, as DFT-C is parameterized almost entirely at the LSDA level of theory, with only the overall scaling parameter changing from $\sigma = 1$ to $\sigma = 0.9$. On the other hand, gCP is parameterized at the GGA level, specifically with B3LYP. It is still true that use of gCP is significantly better than no correction at all.

In Fig. 6, we further assess the transferability of the gCP and DFT-C BSSE correction schemes across three distinct meta-GGAs: a pure meta-GGA B97M-V, a global hybrid M06-2X, and a range-separated hybrid ωB97M-V. Again, we see that across the three meta-GGA functionals, the relative performances of gCP and DFT-C are similar: for all three functionals, gCP exhibits NRMSEs of around 35% for NCED, 50% for NCD, and 60% for NCEC; the corresponding NRMSEs for DFT-C are 25%, 35%, and 20%. Similarly, we see the same sort of consistency for the DFT-C approach at the meta-GGA level as was seen at the GGA and LSDA levels (cf. Figures 5 and 4). On the other hand, gCP is slightly worse at describing molecular clusters at the meta-GGA level than it was at the GGA level. Again, this can be traced back to the facts that gCP systematically overpredicts BSSE in molecular clusters and *meta*-GGA BSSEs tend to be even lower than their GGA counterparts. This overcorrection by gCP can in turn be attributed to its strictly pairwise nature; owing to the inclusion of a many-body

correction, the DFT-C approach does not suffer from this overcounting issue. Note that both gCP and DFT-C can be applied here without modification even to the Minnesota family of density functionals—which are renowned for their non-intuitive and slow convergence of BSSE[108,109]—since the def2-SVPD basis set is too small to capture the unphysical behavior of some of the inhomogeneity correction factors. This same transferability would not be expected in larger, e.g., triple-zeta, basis sets.

Across the seven density functionals examined, the average NRMSE of the DFT-C approach across NCED is 30%, compared to the 42% of gCP; this corresponds to an improvement of more than 25%. For the NCD datatype, the gCP average NRMSE is 59%, compared to 38%—an improvement of 35%. Across the NCEC set of molecular clusters, we see a 46% improvement for DFT-C over gCP: a reduction in average NRMSE from 52% to 28%. It is clear that for a wide variety of systems, across a diverse set of density functionals, in the def2-SVPD basis, the DFT-C method is satisfactorily transferable and represents a significant improvement over gCP for the reproduction of Boys-Bernardi BSSEs. The remaining DFT-C error of course represents the remaining gap to perfect reproduction of the Boys-Bernardi counterpoise correction.

Thus far, with the exception of the basis set comparison in Fig. 3, all errors have been expressed relative to "exact" BSSEs. Although such metrics are relevant for this particular work, since the DFT-C and gCP methods are designed and trained to reproduce BSSEs, they are not of the same broad interest as, say, errors relative to high-level electronic structure methods. In Fig. 7, we show root-mean-square errors (RMSEs) across the five datatypes from
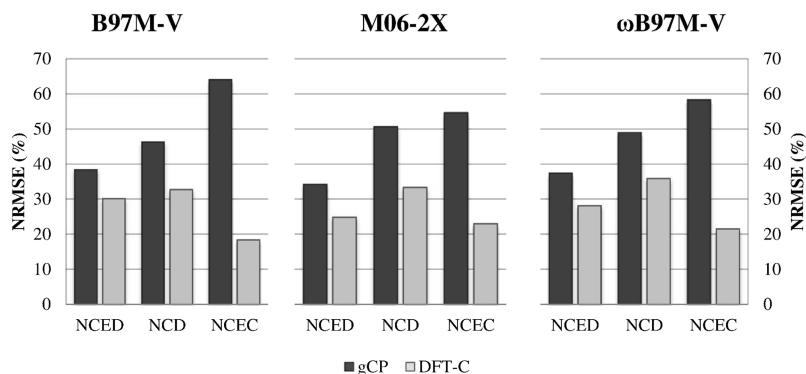

FIG. 6. Normalized root-mean-square errors (NRMSEs) of gCP and DFT-C predicted BSSEs versus Boys and Bernardi BSSEs for three meta-GGA density functionals in the def2-SVPD basis. For further details, see Fig. 4.
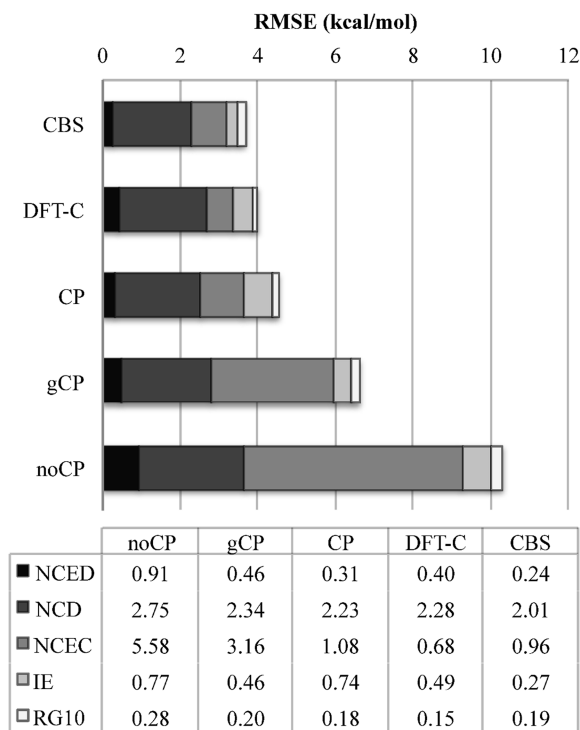
FIG. 7. Root-mean-square errors of B97M-V versus high-level reference values at five levels of theory: uncorrected in the def2-SVPD basis (noCP); counterpoise-corrected in def2-SVPD (CP); with the geometrical counterpoise correction in def2-SVPD (gCP); with the correction introduced in this work in the def2-SVPD basis (DFT-C); and near the complete-basis set limit (CBS), in def2-QZVPPD. Methods in the chart are ordered from lowest overall RMSE at the top to highest overall RMSE at the bottom. A table of values is provided below the chart to facilitate quantitative comparison.

Table I for the B97M-V functional relative to high-level (generally CCSD(T)/CBS) results. The noCP and CP designations correspond to uncorrected and counterpoise-corrected B97M-V/def2-SVPD, respectively, and CBS corresponds to B97M-V/def2-QZVPPD—effectively B97M-V at the basis set limit. DFT-C and gCP refer to B97M-V/def2-SVPD with the corresponding approximation for BSSE included.

From Fig. 7, it is immediately evident that any sort of BSSE correction is preferable to no correction. By correcting using the standard Boys-Bernardi approach, we are able to eliminate 90% of basis set error for NCED, 71% for NCD, 97% for NCEC, and even improve upon CBS results for RG10. Unfortunately, the standard counterpoise correction cannot be applied for the vast majority of isomerization energies—it can only be applied for relative energies, such as relative binding energies—and so the CP and noCP results are almost identical for IE. On the other hand, both gCP and DFT-C offer solid improvements over noCP for every datatype examined, including isomerization energies, for which we are able to eliminate roughly 60% of basis set error. Errors across the individual datasets comprising each aggregate datatype are provided in Fig. 8.

From Fig. 8, it is apparent that there exist datasets in NCED for which gCP outperforms DFT-C; likewise, DFT-C outperforms gCP on a subset of IE. Nevertheless, for B97M-V/def2-SVPD, the DFT-C approach generally offers modest improvements over gCP for molecular dimers (NCED, NCD, and RG10), a significant improvement for molecular

Dataset	noCP	CP	DFT-C	gCP
S66	1.22	0.20	0.34	0.41
A24	0.52	0.17	0.26	0.24
DS14	0.86	0.16	0.27	0.29
HB15	0.82	0.28	0.36	0.34
HSG	0.87	0.14	0.38	0.42
NBC10	1.19	0.37	0.42	0.27
S22	1.57	0.34	0.50	0.45
X31	1.02	0.21	0.29	0.42
A21x12	0.30	0.10	0.18	0.17
BzDC215	0.70	0.28	0.28	0.26
HW30	0.62	0.14	0.20	0.17
NC15	0.43	0.10	0.23	0.25
S66x8	0.95	0.25	0.36	0.42
3B-69-DIM	1.01	0.26	0.32	0.38
AlkBind12	1.34	0.20	0.73	0.60
CO2Nitrogen16	0.94	0.21	0.46	0.31
HB49	0.85	0.41	0.58	0.64
Ionic43	1.27	1.11	1.41	1.90
TA13	4.92	4.64	4.61	4.58
XB18	2.09	1.20	1.41	1.51
Bauza30	2.60	1.94	2.00	2.13
CT20	0.92	0.32	0.51	0.53
XB51	2.43	1.51	1.66	1.80
H2O6Bind8	3.28	0.22	0.51	1.57
HW6Cl	2.64	0.44	0.84	1.42
HW6F	2.78	0.52	0.54	1.94
FmH2O10	9.53	0.33	0.64	5.66
Shields38	4.05	0.22	0.44	1.84
SW49Bind345	1.17	1.17	0.35	1.39
SW49Bind6	2.51	2.51	0.68	2.83
Water27	3.27	1.08	0.96	1.61
H2O20Bind4	18.11	0.49	1.83	8.75
3B-69-TRIM	2.66	0.54	0.70	0.89
CE20	2.84	0.55	0.64	1.37
H2O20Bind10	18.72	2.63	0.58	11.23
AlkIsomer11	0.46	0.46	0.37	0.36
Butanediol65	0.37	0.37	0.18	0.12
ACONF	0.21	0.21	0.12	0.11
CYCONF	0.17	0.17	0.19	0.14
Pentane14	0.07	0.07	0.15	0.11
SW49Rel345	0.36	0.36	0.34	0.41
SW49Rel6	0.38	0.38	0.42	0.70
H2O16Rel5	1.44	1.44	1.02	0.36
H2O20Rel10	0.82	0.13	0.64	0.39
H2O20Rel4	2.59	0.49	1.88	0.62
Melatonin52	0.73	0.73	0.49	0.70
YMPJ519	0.83	0.83	0.51	0.47
RG10	0.28	0.18	0.15	0.20

FIG. 8. Root-mean-square errors of B97M-V/def2-SVPD versus "exact" reference values with no correction (noCP), the standard counterpoise correction (CP), the geometrical counterpoise correction (gCP), and the treatment introduced here (DFT-C). All RMSEs are in units of kcal/mol. Each row is color-coded for ease of reading, with darker cells corresponding to lower RMSEs. From top to bottom, the blocks correspond to the NCED, NCD, NCEC, IE, and RG10 datatypes. Note for SW49 and most of IE, the standard counterpoise correction is not possible, and so for these datasets the noCP and CP methods are identical.

clusters (NCEC), and is slightly inferior for isomerization energies (IE). The DFT-C method outperforms the Boys-Bernardi counterpoise correction across the full dataset, with an overall RMSE of 0.56 kcal/mol compared to a CP RMSE of 0.63 RMSE; the large improvement it affords for NCEC and IE offset the small losses on NCED and NCD. As such, DFT-C is a viable alternative to the traditional counterpoise correction in the def2-SVPD basis set, yielding similar results to CP with effectively no increase in cost over noCP.

To further illustrate the power of the DFT-C BSSE-correction scheme, in Fig. 9, we show RMSEs across the

Functional	Datatype			
(Basis)	NCED	NCD	NCEC	IE
B97M-V (SVPD)	0.91	2.75	5.58	0.77
B97M-V-C (SVPD)	0.40	2.28	0.68	0.49
B97M-V (QZVPPD)	0.24	2.01	0.96	0.27
M06-L (QZVPPD)	0.55	1.87	2.20	0.71
TM (QZVPPD)	0.50	3.13	1.59	0.49
MS2-D3(op) (QZVPPD)	0.29	2.65	0.89	0.35

FIG. 9. Root-mean-square errors in kcal/mol of several pure meta-GGA density functionals relative to high-level reference values. B97M-V-C corresponds to B97M-V with the DFT-C correction. Results for the additional density functionals are taken from a previous study.[111] SVPD corresponds to def2-SVPD and QZVPPD corresponds to def2-QZVPPD. Each datatype category is color-coded, with the darkest color corresponding to the lowest RMSE within that category.

four aggregate datatypes for B97M-V with (B97M-V-C) and without (B97M-V) the DFT-C correction for BSSE in the def2-SVPD basis, as well as for four popular pure meta-GGA density functionals—B97M-V,[104] MS2-D3(op),[110,111] M06-L,[112] and TM[113]—near the CBS limit, in the def2-QZVPPD basis. From Fig. 9, it is clear that although B97M-V/def2-SVPD is not competitive with standard meta-GGAs at the basis set limit, B97M-V-C/def2-SVPD certainly is—despite requiring a small fraction of the computational effort.

IV. DISCUSSION AND CONCLUSIONS

In this study, we have introduced a physically motivated empirical correction for basis set superposition error within the def2-SVPD basis set: DFT-C. This correction differs from the existing gCP approach—which we have also re-parameterized for use in the def2-SVPD basis—in two critical areas. First, whereas the linear coefficients within gCP include all manifestations of basis set incompleteness error, the DFT-C approach is constructed exclusively from basis set superposition errors. Second, although gCP is a strictly pairwise correction, in DFT-C, each pairwise contribution is reduced by a many-body term to ameliorate the overcounting concomitant with the non-orthogonality of the Hilbert spaces of nearby atoms. We have evaluated both gCP and DFT-C across a diverse dataset containing 3402 non-covalent interactions and isomerization energies.

This new method, DFT-C, yields significantly more accurate BSSEs than gCP for a wide variety of interaction motifs. Moreover, the correction is transferable. DFT-C exhibits roughly the same relative performances across the various non-covalent datatypes regardless of the particular density functional with which it is paired: for non-covalently interacting dimers, DFT-C offers a modest improvement over gCP; in the case of molecular clusters—particularly when a

meta-GGA functional is employed—the improvement is more pronounced, which is likely attributable to the many-body nature of the method.

Whereas gCP has been developed as a general purpose tool that can be relatively easily adapted to any basis set, the DFT-C approach is much more complicated and specialized; tabulating the many pairwise coefficients and decay parameters is a nontrivial task. In this particular work, we have introduced a correction for def2-SVPD, a double-zeta basis set that has disproportionately low intrinsic basis set incompleteness error for how few basis functions it contains.[38] We are also exploring the possibility of extending this method to triple-zeta basis sets in order to truly push the basis set limit; such may be the focus of work to come. Additionally, we are exploring the impact of the DFT-C correction on thermochemical energies and equilibrium geometries.

The gCP correction is an integral component of the small-basis functional PBEh-3c. The DFT-C correction could be incorporated in a similar fashion into a composite small-basis method by allowing some subset of the linear parameters, c_A—or simply the overall scaling parameter σ—to vary. Even without modification, however, the method is immensely powerful; we have demonstrated that it can be paired with an existing functional, B97M-V, to yield def2-SVPD results on par with def2-QZVPPD results for other state-of-the-art pure meta-GGA density functionals. DFT-C should prove immensely useful for recovering large-basis results for many energetic properties with small-basis effort—the correction scales with the number of atoms, not the number of basis functions, after all, and is essentially free on the scale of an electronic structure calculation—and it can be paired without modification with any density functional. This could allow us to obtain high-quality results for large systems which are currently out of the domain of quantitative electronic structure theory.

SUPPLEMENTARY MATERIAL

See supplementary material for the simple Python implementation of the DFT-C method, as well as parameterizations for both DFT-C and gCP within the def2-SVPD basis and several additional tables and figures.

ACKNOWLEDGMENTS

[1]H. B. Jansen and P. Ros, Chem. Phys. Lett. **3**, 140 (1969).
[2]S. Boys and F. Bernardi, Mol. Phys. **19**, 553 (1970).
[3]B. Liu and A. D. McLean, J. Chem. Phys. **59**, 4557 (1973).
[4]B. Brauer, M. K. Kesharwani, and J. M. L. Martin, J. Chem. Theory Comput. **10**, 3791 (2014).

[5]D. R. Bowler and T. Miyazaki, J. Phys.: Condens. Matter **22**, 074207 (2010).

[6]C.-K. Skylaris, P. D. Haynes, A. A. Mostofi, and M. C. Payne, J. Chem. Phys. **122**, 084119 (2005).

[7]C.-K. Skylaris, P. D. Haynes, A. A. Mostofi, and M. C. Payne, J. Phys.: Condens. Matter **20**, 064209 (2008).

[8]M. J. Rayson and P. R. Briddon, Phys. Rev. B **80**, 205104 (2009).

[9]M. Rayson, Comput. Phys. Commun. **181**, 1051 (2010).

[10]Y. Mao, P. R. Horn, N. Mardirossian, T. Head-Gordon, C.-K. Skylaris, and M. Head-Gordon, J. Chem. Phys. **145**, 044109 (2016).

[11]D. W. Schwenke and D. G. Truhlar, J. Chem. Phys. **82**, 2418 (1985).

[12]J. Collins and G. Gallup, Chem. Phys. Lett. **123**, 56 (1986).

[13]M. J. Frisch, J. E. Del Bene, J. S. Binkley, and H. F. Schaefer III, J. Chem. Phys. **84**, 2279 (1986).

[14]M. Gutowski, F. Van Duijneveldt, G. Chałasiński, and L. Piela, Chem. Phys. Lett. **129**, 325 (1986).

[15]D. B. Cook, J. A. Sordo, and T. L. Sordo, Int. J. Quantum Chem. **48**, 375 (1993).

[16]F. B. van Duijneveldt, J. G. C. M. van Duijneveldt-van de Rijdt, and J. H. van Lenthe, Chem. Rev. **94**, 1873 (1994).

[17]M. Mentel and E. J. Baerends, J. Chem. Theory Comput. **10**, 252 (2014).

[18]R. Kalescky, E. Kraka, and D. Cremer, J. Chem. Phys. **140**, 084315 (2014).

[19]E. Miliordos and S. S. Xantheas, J. Chem. Phys. **142**, 094311 (2015).

[20]L. A. Burns, M. S. Marshall, and C. D. Sherrill, J. Chem. Theory Comput. **10**, 49 (2014).

[21]R. Z. Khaliullin, M. Head-Gordon, and A. T. Bell, J. Chem. Phys. **124**, 204105 (2006).

[22]P. R. Horn, E. J. Sundstrom, T. A. Baker, and M. Head-Gordon, J. Chem. Phys. **138**, 134119 (2013).

[23]A. Galano and J. R. Alvarez-Idaboy, J. Comput. Chem. **27**, 1203 (2006); e-print arXiv:NIHMS150003.

[24]F. Jensen, J. Chem. Theory Comput. **6**, 100 (2010).

[25]J. C. Faver, Z. Zheng, and K. M. Merz, J. Chem. Phys. **135**, 144110 (2011).

[26]J. C. Faver, Z. Zheng, and K. M. Merz, Phys. Chem. Chem. Phys. **14**, 7795 (2012).

[27]H. Kruse and S. Grimme, J. Chem. Phys. **136**, 154101 (2012).

[28]S. Grimme, J. Antony, S. Ehrlich, and H. Krieg, J. Chem. Phys. **132**, 154104 (2010).

[29]S. Grimme, S. Ehrlich, and L. Goerigk, J. Comput. Chem. **32**, 1456 (2011).

[30]R. Sure and S. Grimme, J. Comput. Chem. **34**, 1672 (2013).

[31]S. Grimme, J. G. Brandenburg, C. Bannwarth, and A. Hansen, J. Chem. Phys. **143**, 054107 (2015).

[32]J. G. Brandenburg, E. Caldeweyher, and S. Grimme, Phys. Chem. Chem. Phys. **18**, 15519 (2016).

[33]H. Kruse, L. Goerigk, and S. Grimme, J. Organic Chem. **77**, 10824 (2012).

[34]L. Goerigk and J. R. Reimers, J. Chem. Theory Comput. **9**, 3240 (2013).

[35]L. Goerigk, J. Chem. Theory Comput. **10**, 968 (2014).

[36]F. Weigend and R. Ahlrichs, Phys. Chem. Chem. Phys. **7**, 3297 (2005).

[37]D. Rappoport and F. Furche, J. Chem. Phys. **133**, 134105 (2010).

[38]J. Witte, J. B. Neaton, and M. Head-Gordon, J. Chem. Phys. **144**, 194306 (2016).

[39]C. C. J. Roothaan, Rev. Mod. Phys. **32**, 179 (1960).

[40]F. Jensen, J. Chem. Phys. **115**, 9113 (2001).

[41]F. Jensen, J. Chem. Phys. **116**, 7372 (2002).

[42]F. Jensen, J. Chem. Phys. **117**, 9234 (2002).

[43]A. Becke, Phys. Rev. A **38**, 3098 (1988).

[44]C. Lee, W. Yang, and R. Parr, Phys. Rev. B **37**, 785 (1988).

[45]A. D. Becke, J. Chem. Phys. **98**, 5648 (1993).

[46]P. Stephens, F. Devlin, C. Chabalowski, and M. Frisch, J. Phys. Chem. **98**, 11623 (1994).

[47]J. Řezáč, K. E. Riley, and P. Hobza, J. Chem. Theory Comput. **7**, 2427 (2011).

[48]B. Brauer, M. K. Kesharwani, S. Kozuch, and J. M. L. Martin, Phys. Chem. Chem. Phys. **18**, 20905 (2016).

[49]M. M. Morrell, R. G. Parr, and M. Levy, J. Chem. Phys. **62**, 549 (1975).

[50]A. D. Dutoi and M. Head-Gordon, J. Phys. Chem. A **112**, 2110 (2008).

[51]P. Hohenberg and W. Kohn, Phys. Rev. **136**, B864 (1964).

[52]W. Kohn and L. Sham, Phys. Rev. **140**, A1133 (1965).

[53]J. C. Slater, *The Self-Consistent Field for Molecules and Solids, Quantum Theory of Molecules and Solids* (McGraw-Hill, New York, 1974).

[54]J. Perdew and Y. Wang, Phys. Rev. B **45**, 13244 (1992).

[55]N. Mardirossian and M. Head-Gordon, J. Chem. Phys. **144**, 214110 (2016).

[56]J. Řezáč, K. E. Riley, and P. Hobza, J. Chem. Theory Comput. **7**, 3466 (2011).

[57]J. Řezáč and P. Hobza, J. Chem. Theory Comput. **9**, 2151 (2013).

[58]B. J. Mintz and J. M. Parks, J. Phys. Chem. A **116**, 1086 (2012).

[59]J. Řezáč, K. E. Riley, and P. Hobza, J. Chem. Theory Comput. **8**, 4285 (2012).

[60]J. C. Faver, M. L. Benson, X. He, B. P. Roberts, B. Wang, M. S. Marshall, M. R. Kennedy, C. D. Sherrill, and K. M. Merz, J. Chem. Theory Comput. **7**, 790 (2011); e-print arXiv:NIHMS150003.

[61]M. S. Marshall, L. A. Burns, and C. D. Sherrill, J. Chem. Phys. **135**, 194102 (2011).

[62]E. G. Hohenstein and C. D. Sherrill, J. Phys. Chem. A **113**, 878 (2009).

[63]C. D. Sherrill, T. Takatani, and E. G. Hohenstein, J. Phys. Chem. A **113**, 10146 (2009).

[64]T. Takatani and C. David Sherrill, Phys. Chem. Chem. Phys. **9**, 6106 (2007).

[65]P. Jurecka, J. Sponer, J. Cerný, and P. Hobza, Phys. Chem. Chem. Phys. **8**, 1985 (2006).

[66]J. Řezáč and P. Hobza, J. Chem. Theory Comput. **8**, 141 (2012).

[67]J. Witte, M. Goldey, J. B. Neaton, and M. Head-Gordon, J. Chem. Theory Comput. **11**, 1481 (2015).

[68]D. L. Crittenden, J. Phys. Chem. A **113**, 1663 (2009).

[69]K. L. Copeland and G. S. Tschumper, J. Chem. Theory Comput. **8**, 1646 (2012).

[70]D. G. A. Smith, P. Jankowski, M. Slawik, H. A. Witek, and K. Patkowski, J. Chem. Theory Comput. **10**, 3140 (2014).

[71]J. Řezáč, Y. Huang, P. Hobza, and G. J. O. Beran, J. Chem. Theory Comput. **11**, 3065 (2015).

[72]S. Li, D. G. A. Smith, and K. Patkowski, Phys. Chem. Chem. Phys. **17**, 16560 (2015).

[73]K. U. Lao and J. M. Herbert, J. Phys. Chem. A **119**, 235 (2015).

[74]A. D. Boese, J. Chem. Theory Comput. **9**, 4403 (2013).

[75]A. D. Boese, Mol. Phys. **113**, 1618 (2015).

[76]A. D. Boese, ChemPhysChem **16**, 978 (2015).

[77]J. Granatier, M. Pitoňák, and P. Hobza, J. Chem. Theory Comput. **8**, 2282 (2012).

[78]K. U. Lao and J. M. Herbert, J. Chem. Phys. **139**, 034107 (2013).

[79]K. U. Lao, R. Schäffer, G. Jansen, and J. M. Herbert, J. Chem. Theory Comput. **11**, 2473 (2015).

[80]B. Temelso, K. A. Archer, and G. C. Shields, J. Phys. Chem. A **115**, 12034 (2011).

[81]N. Mardirossian, D. S. Lambrecht, L. McCaslin, S. S. Xantheas, and M. Head-Gordon, J. Chem. Theory Comput. **9**, 1368 (2013).

[82]V. S. Bryantsev, M. S. Diallo, A. C. T. Van Duin, and W. A. Goddard, J. Chem. Theory Comput. **5**, 1016 (2009).

[83]L. Goerigk and S. Grimme, J. Chem. Theory Comput. **6**, 107 (2010).

[84]G. S. Fanourgakis, E. Aprà, and S. S. Xantheas, J. Chem. Phys. **121**, 2655 (2004).

[85]T. Anacker and J. Friedrich, J. Comput. Chem. **35**, 634 (2014).

[86]A. Karton, R. J. O'Reilly, B. Chan, and L. Radom, J. Chem. Theory Comput. **8**, 3128 (2012).

[87]B. Chan, A. T. B. Gilbert, P. M. W. Gill, and L. Radom, J. Chem. Theory Comput. **10**, 3777 (2014).

[88]P. R. Tentscher and J. S. Arey, J. Chem. Theory Comput. **9**, 1568 (2013).

[89]S. Kozuch and J. M. L. Martin, J. Chem. Theory Comput. **9**, 1918 (2013).

[90]A. Bauzá, I. Alkorta, A. Frontera, and J. Elguero, J. Chem. Theory Comput. **9**, 5201 (2013).

[91]A. Otero-de-la-Roza, E. R. Johnson, and G. A. DiLabio, J. Chem. Theory Comput. **10**, 5436 (2014).

[92]S. N. Steinmann, C. Piemontesi, A. Delachat, and C. Corminboeuf, J. Chem. Theory Comput. **8**, 1629 (2012).

[93]A. Karton, D. Gruzman, and J. M. L. Martin, J. Phys. Chem. A **113**, 8434 (2009); e-print arXiv:0905.3271.

[94]S. Kozuch, S. M. Bachrach, and J. M. L. Martin, J. Phys. Chem. A **118**, 293 (2014).

[95]D. Gruzman, A. Karton, and J. M. L. Martin, J. Phys. Chem. A **113**, 11974 (2009).

[96]J. J. Wilke, M. C. Lind, H. F. Schaefer, A. G. Csaszar, and W. D. Allen, J. Chem. Theory Comput. **5**, 1511 (2009).

[97]J. M. L. Martin, J. Phys. Chem. A **117**, 3118 (2013).

[98]S. Yoo, E. Aprà, X. C. Zeng, and S. S. Xantheas, J. Phys. Chem. Lett. **1**, 3122 (2010).

[99]U. R. Fogueri, S. Kozuch, A. Karton, and J. M. L. Martin, J. Phys. Chem. A **117**, 2269 (2013).

[100]M. K. Kesharwani, A. Karton, and J. M. L. Martin, J. Chem. Theory Comput. **12**, 444 (2016).
[101]K. T. Tang and J. P. Toennies, J. Chem. Phys. **118**, 4976 (2003).
[102]J. P. Perdew, K. Burke, and M. Ernzerhof, Phys. Rev. Lett. **77**, 3865 (1996).
[103]N. Mardirossian and M. Head-Gordon, Phys. Chem. Chem. Phys. **16**, 9904 (2014).
[104]N. Mardirossian and M. Head-Gordon, J. Chem. Phys. **142**, 074111 (2015).
[105]Y. Zhao and D. G. Truhlar, Theor. Chem. Acc. **120**, 215 (2008).
[106]P. M. Gill, B. G. Johnson, and J. A. Pople, Chem. Phys. Lett. **209**, 506 (1993).
[107]Y. Shao, Z. Gan, E. Epifanovsky, A. T. Gilbert, M. Wormit, J. Kussmann, A. W. Lange, A. Behn, J. Deng, X. Feng, D. Ghosh, M. Goldey, P. R. Horn, L. D. Jacobson, I. Kaliman, R. Z. Khaliullin, T. Kuś, A. Landau, J. Liu, E. I. Proynov, Y. M. Rhee, R. M. Richard, M. A. Rohrdanz, R. P. Steele, E. J. Sundstrom, H. L. Woodcock, P. M. Zimmerman, D. Zuev, B. Albrecht, E. Alguire, B. Austin, G. J. O. Beran, Y. A. Bernard, E. Berquist, K. Brandhorst, K. B. Bravaya, S. T. Brown, D. Casanova, C.-M. Chang, Y. Chen, S. H. Chien, K. D. Closser, D. L. Crittenden, M. Diedenhofen, R. A. DiStasio, H. Do, A. D. Dutoi, R. G. Edgar, S. Fatehi, L. Fusti-Molnar, A. Ghysels, A. Golubeva-Zadorozhnaya, J. Gomes, M. W. Hanson-Heine, P. H. Harbach, A. W. Hauser, E. G. Hohenstein, Z. C. Holden, T.-C. Jagau, H. Ji, B. Kaduk, K. Khistyaev, J. Kim, J. Kim, R. A. King, P. Klunzinger, D. Kosenkov, T. Kowalczyk, C. M. Krauter, K. U. Lao, A. D. Laurent, K. V. Lawler, S. V. Levchenko, C. Y. Lin, F. Liu, E. Livshits, R. C. Lochan, A. Luenser, P. Manohar, S. F. Manzer, S.-P. Mao, N. Mardirossian, A. V. Marenich, S. A. Maurer, N. J. Mayhall, E. Neuscamman, C. M. Oana, R. Olivares-Amaya, D. P. O'Neill, J. A. Parkhill, T. M. Perrine, R. Peverati, A. Prociuk, D. R. Rehn, E. Rosta, N. J. Russ, S. M. Sharada, S. Sharma, D. W. Small, A. Sodt, T. Stein, D. Stück, Y.-C. Su, A. J. Thom, T. Tsuchimochi, V. Vanovschi, L. Vogt, O. Vydrov, T. Wang, M. A. Watson, J. Wenzel, A. White, C. F. Williams, J. Yang, S. Yeganeh, S. R. Yost, Z.-Q. You, I. Y. Zhang, X. Zhang, Y. Zhao, B. R. Brooks, G. K. Chan, D. M. Chipman, C. J. Cramer, W. A. Goddard, M. S. Gordon, W. J. Hehre, A. Klamt, H. F. Schaefer, M. W. Schmidt, C. D. Sherrill, D. G. Truhlar, A. Warshel, X. Xu, A. Aspuru-Guzik, R. Baer, A. T. Bell, N. A. Besley, J.-D. Chai, A. Dreuw, B. D. Dunietz, T. R. Furlani, S. R. Gwaltney, C.-P. Hsu, Y. Jung, J. Kong, D. S. Lambrecht, W. Liang, C. Ochsenfeld, V. A. Rassolov, L. V. Slipchenko, J. E. Subotnik, T. Van Voorhis, J. M. Herbert, A. I. Krylov, P. M. Gill, and M. Head-Gordon, Mol. Phys. **113**, 184 (2015).
[108]N. Mardirossian and M. Head-Gordon, J. Chem. Theory Comput. **9**, 4453 (2013).
[109]L. Goerigk, J. Phys. Chem. Lett. **6**, 3891 (2015).
[110]J. Sun, R. Haunschild, B. Xiao, I. W. Bulik, G. E. Scuseria, and J. P. Perdew, J. Chem. Phys. **138**, 044113 (2013); e-print arXiv:1301.2239v1.
[111]J. Witte, N. Mardirossian, J. B. Neaton, and M. Head-Gordon, J. Chem. Theory Comput. **13**, 2043 (2017).
[112]Y. Zhao and D. G. Truhlar, J. Chem. Phys. **125**, 194101 (2006).
[113]J. Tao and Y. Mo, Phys. Rev. Lett. **117**, 73001 (2016).